

# Magnetoresistance, temporal evolution, and relaxation of the electrical resistivity in the re-entrant semiconducting $\text{La}_{0.80}\text{Ba}_{0.20}\text{CoO}_3$ perovskite

R. D. Sánchez,<sup>a)</sup> J. Mira, and J. Rivas

*Dpto. Física Aplicada, Universidad de Santiago de Compostela, 15706 Santiago de Compostela, Spain*

M. P. Breijo and M. A. Señas-Rodríguez<sup>b)</sup>

*Dpto. Química Fundamental e Industrial, Universidad de A Coruña, 15071 A Coruña, Spain*

(Received 26 January 1998; accepted 12 February 1999)

We report here a study on the electrical and magnetic properties of  $\text{La}_{1-x}\text{Ba}_x\text{CoO}_3$  in the re-entrant semiconducting region ( $x = 0.20$ ). We find that in this material: (i) the insulator-metal-insulator sequence is unstable and evolves toward a purely semiconducting behavior; the initial  $\rho$  versus  $T$  curve can be reinstated upon appropriate annealing treatments; (ii) there are relaxation effects that can be seen by changing the polarity of the electrodes; (iii) there is a negative magnetoresistance  $\Delta\rho/\rho \sim 2\text{--}3\%$ , for a field as low as 9 kOe, especially at the metal-insulating transition temperatures; and (iv) there are important fluctuations in the electrical resistivity. Taking into account these experimental observations, we can interpret this material as an inhomogeneous system where two thermodynamic phases, one semiconducting and the other metallic and ferromagnetic, coexist, although they are crystallographically indistinguishable.

## I. INTRODUCTION

Early studies on the magnetic and electrical properties of magnetic semiconductors such as EuSe and EuTe showed that their particular properties can be described as a consequence of their heterogeneity due to a two-phase segregation. This segregation forms ferromagnetic (FM) microregions (called ferrons, giant quasimolecules, or magnetic polarons) within an antiferromagnetic (AF,  $T < T_N$ ) or paramagnetic (PM,  $T > T_N$ ) phase.<sup>1</sup> This idea was used by some authors to explain the peculiar transport properties in the copper oxide superconductors.<sup>1,2</sup> More recently, it has been used to interpret the colossal magnetoresistance observed in manganese perovskites near the Curie temperature.<sup>3–5</sup>

Another perovskite system where a phase segregation has been reported is  $\text{La}_{1-x}\text{Sr}_x\text{CoO}_3$ . The extreme member of the series with  $x = 0$ ,  $\text{LaCoO}_3$ , shows peculiar magnetic and transport properties due to a thermally induced spin transition from low-spin Co(III) ( $t_2^6 e^0$ ) to mostly high-spin  $\text{Co}^{3+}$  ( $t_2^4 e^2$ ).<sup>6–8</sup> The complete evolution and interpretation of both its electrical and magnetic properties as a function of temperature have been recently revised.<sup>9</sup>

Upon Sr doping, very noticeable changes take place in the material<sup>10</sup>: while  $\text{LaCoO}_3$  shows high resistivity

and antiferromagnetic exchange interactions, the materials  $\text{La}_{1-x}\text{Sr}_x\text{CoO}_3$  evolve toward a metallic ferromagnetic behavior. According to an earlier interpretation,<sup>11</sup> in the doped samples paramagnetic  $\text{La}^{3+}$  coexisted with ferromagnetic  $\text{Sr}^{2+}$ -rich clusters, the ferromagnetic component increasing with  $x$ . Re-examination of this system has led some authors to propose a phase diagram for the electronic structure of this very complex system.<sup>12</sup> According to their interpretation, upon  $\text{Sr}^{2+}$  doping the material segregates into two distinguishable electronic states that coexist within the same crystallographic phase: hole-rich metallic ferromagnetic regions, where the Co ions are in an intermediate-spin configuration, and a hole-poor matrix similar to  $\text{LaCoO}_3$  which experiences a thermally induced low-spin to high-spin transition. For low Sr contents  $x < 0.20$  the hole-rich regions are isolated from one another and show spin-glass behavior at  $T < T_g$  and the samples are semiconducting. For high enough Sr contents,  $x \geq 0.30$ , magnetic and electrical percolation are achieved and the samples are metallic and ferromagnetic. For intermediate compositions the authors reported bulk ferromagnetism below  $T_C$  and insulator-metal-insulator transitions (I-M-I), also known as re-entrant semiconducting behavior (RSB), as temperature rises.

In order to gain insight into the peculiarities of that re-entrant semiconducting region and into other effects due to the presence of two phases, we have carried out magnetic and electrical studies on  $\text{La}_{1-x}\text{B}_x\text{CoO}_3$  systems, with (B = Ca, Sr, and Ba) that show RSB. In

<sup>a)</sup>Permanent address: Centro Atómico de Bariloche–Carrera de Investigador del CONICET (Argentina).

<sup>b)</sup>Address all correspondence to this author. e-mail: tonasr@udc.es

this paper we focus our study on one of these materials:  $\text{La}_{1-x}\text{Ba}_x\text{CoO}_3$  with  $x = 0.2$ .

## II. EXPERIMENTAL

$\text{La}_{0.80}\text{Ba}_{0.20}\text{CoO}_3$  was prepared by decomposition of the corresponding mixture of nitrates. Stoichiometric amounts of dry  $\text{La}_2\text{O}_3$  and  $\text{BaCO}_3$  were dissolved in nitric acid and mixed with the appropriate volume of a cobalt nitrate solution prepared and standardized, as reported in Ref. 9. The resulting solution was warmed up so as to slowly evaporate the solvent. The so-obtained mixture of nitrates was decomposed at 600 °C. The resulting product was pressed into pellets and was then annealed at 1000–1100 °C/79 h and cooled slowly to room temperature at 60 °C/h.

The so-obtained Ba compound was crystalline and single phase, as shown by its x-ray powder diffraction pattern obtained from a SIEMENS D-50000 apparatus. Scanning electron micrographs showed the microstructure of sintered grains. The final grain size is approximately 2  $\mu\text{m}$ .

The magnetic properties were studied in a VSM vibrating magnetometer. Zero-field-cool (ZFC) and field-cool (FC) magnetic susceptibility data were obtained in a field of 1 kOe from  $77 \leq T \text{ (K)} \leq 330$ . ZFC and FC magnetization curves  $M(H)$  were obtained using fields of  $\pm 10$  kOe at 77 K, at the temperature where the metal-insulator transition took place in the resistivity versus temperature measurements, and at temperatures slightly below and above  $T_C$ .

The electrical resistivity of bars  $\sim (1 \times 4 \times 8) \text{ mm}^3$  was studied in the temperature interval  $77 \leq T \text{ (K)} \leq 300$  in a four-probe homemade device equipped with a commercial Oxford ITC4 temperature controller, a precision electrical current HP 6181C source, a Keithley 2001 multimeter, and a Hall probe.

Constant dc currents [ $10 \leq I \text{ (mA)} \leq 50$ ], with an error of 0.03%, were applied across the entire cross section (A) of the bar samples through electrodes (copper wires) situated at the ends of the specimen. The voltage was measured in the scale of 200 mV, with a resolution of 10 nV, through two additional electrodes separated by a distance  $d$  and welded in between the former. The electrical resistivity was computed as  $\rho = VA/Id = R_s A/d$ .

The electrical contacts between the electrodes and the sample were mostly made with silver paint, but in some special cases they were replaced by gold sputtered on the samples or by indium contacts.

To check the quality of the voltage contacts, the electrical resistance between them was measured at two ( $R_{2w}$ ) and four ( $R_{4w}$ ) wires. Assuming that  $R_{2w} = 2R_c + R_s$  and that  $R_{4w} = R_s$ , the contact resistance is  $R_c = (R_{2w} - R_{4w})/2$ . The contacts were considered satisfactory only when  $R_c/R_{4w} \leq 20$ .

To eliminate the thermoelectric effect the resistivity data were obtained, as commonly done, calculating the averages  $\rho^+$  and  $\rho^-$  (+ and – stand for the direction of the current) out of 10 values, respectively, and getting an average resistance  $\rho = (\rho^+ + \rho^-)/2$ . But in some cases, as will be shown below, only one polarity of the current was used for the experiments, thus measuring either  $\rho^+$  or  $\rho^-$ .

The temperature dependence of the resistivity,  $\rho$ , was measured in a zero magnetic field ( $H = 0$ ) and under a constant field ( $H = 5$  kOe). The time dependence of  $\rho^+$  and  $\rho^-$  was studied at room temperature by measuring them every second for some minutes. After a time  $t_1$  the polarity of  $I$  was inverted and finally restored after a time  $t_2$ . The magnetoresistance [ $\Delta\rho/\rho = \rho(H) - \rho(0)/\rho(0)$ ] was measured between 0 and 10 kOe, in steps of 100 Oe, at those temperatures where the  $\rho(H)$  versus  $T$  curves, corresponding to  $H = 0$  and  $H = 5$  kOe, showed bigger separation.

## III. RESULTS

When we partially replace  $\text{La}^{3+}$  by  $\text{Ba}^{2+}$  in the cobalt perovskite we find RSB in  $\text{La}_{1-x}\text{Ba}_x\text{CoO}_3$  for  $x = 0.20$ .

This sample shows bulk ferromagnetism below a  $T_C \approx 175$  K [Fig. 1(a)] and typical hysteresis loops with a coercitive magnetic field ( $H_c$ ) of 1200 Oe at 77 K and a remanent magnetization ( $M_r$ ) of 3300 emu/mol. Above 250 K the data can be fitted to a Curie–Weiss law with an effective magnetic moment ( $\mu_{\text{eff}} \approx \sqrt{8C}$ ) of 4.6  $\mu_B$  and a Weiss constant of 155 K. For  $T_C < T \leq 250$  K there is a positive deviation from the Curie–Weiss law [Fig. 1(b)] and hysteresis in the  $M(H)$  measurements with  $H_c < 100$  Oe and  $M_r < 300$  emu/mol.

As for the electrical behavior of this material, Fig. 2 shows  $\rho(T)$  data for the fresh sample (A). The sample is semiconducting below a  $T_{M11}$  and above a  $T_{M12}$ , and metallic for  $T_{M11} < T < T_{M12}$ , as indicated in that figure.

Interestingly enough, the electrical resistivity is observed to evolve with time, as can be seen in the same figure. There we plot  $\rho(T)/\rho(180 \text{ K})$  versus  $T$  in order to compare how the semiconducting re-entrant behavior disappears in the interval of several weeks.

In order to eliminate contact effects as a source of the observed semiconducting behavior, the electrical contacts were changed. Thus, while silver paint contacts were used when measuring the first two times (A and B), after detecting the evolution in B we removed the silver paint contacts with acetone and made four new contacts (C). In order to make the fourth measurement, we removed the previous contacts and, on the opposite face of the pellet, we pressed metallic indium on the wires (D). Other measurements were done sputtering

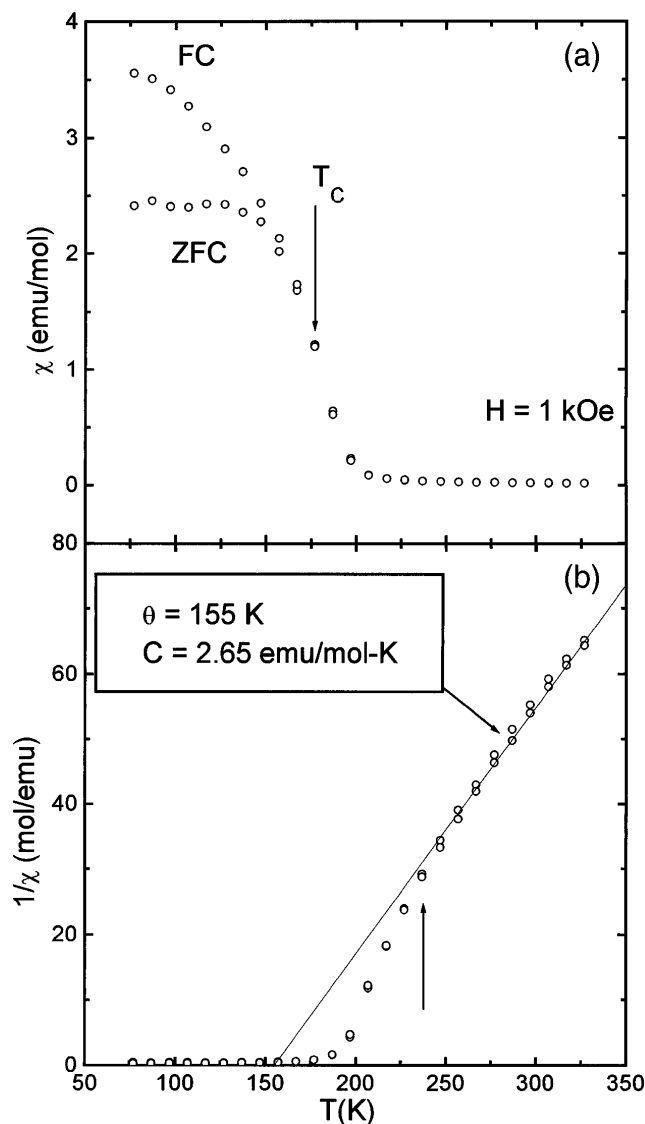


FIG. 1. Magnetic properties of  $\text{La}_{0.80}\text{Ba}_{0.20}\text{CoO}_3$ : (a) ZFC and FC temperature dependence of the molar magnetic susceptibility ( $\chi = M/H$ ). The data were taken with  $H = 1$  kOe. (b) Temperature dependence of the inverse of the susceptibility. Fit of the experimental data to a Curie–Weiss law gives  $\theta = 155$  K and  $C = 2.65$  emu/mol K [ $250 < T$  (K)  $< 330$ ].

gold on the sample and welding the wires by means of silver paint.

It is worth noting at this point that although the electrical properties of this sample clearly vary with time, from the crystallographic point of view the sample does not experience any structural modification, as seen by x-ray powder diffraction (Fig. 3). Also, no changes were observed in its magnetic behavior.

When the aged samples were again thermally treated at the final annealing temperature of synthesis and slowly cooled to room temperature, we could restore the as-prepared  $\rho$  versus  $T$  curve (similar to sample A in Fig. 2).

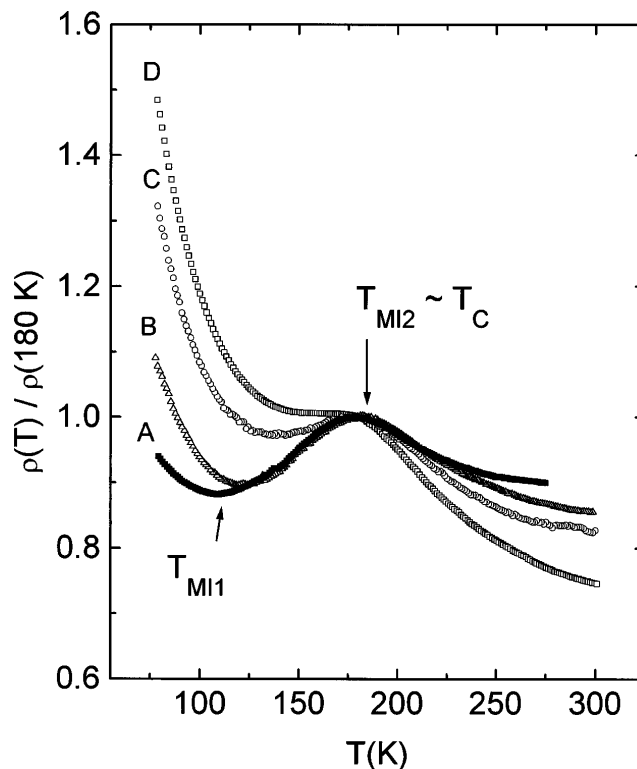


FIG. 2. Normalized electrical resistivity  $\rho(T)/\rho(180 \text{ K})$  of  $\text{La}_{0.80}\text{Ba}_{0.20}\text{CoO}_3$  samples as a function of temperature. The sequence from A to D shows the temporal evolution of the samples every two months. The absolute resistivities measured at 180 K are, approximately,  $\rho_A = 1.38$  mΩ cm,  $\rho_B = 1.61$  mΩ cm,  $\rho_C = 2.63$  mΩ cm, and  $\rho_D = 2.28$  mΩ cm.

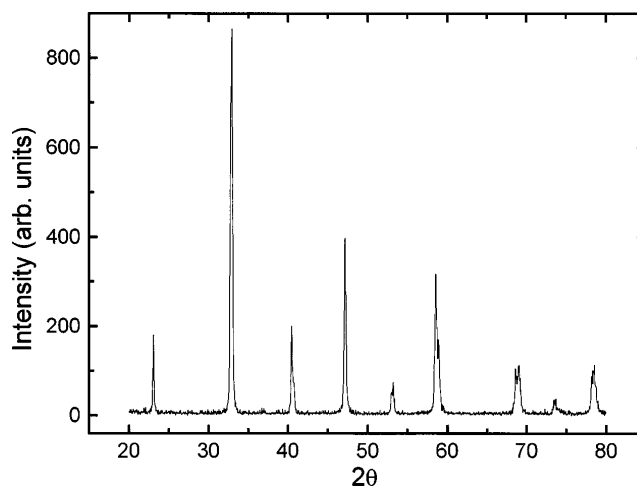


FIG. 3. Powder x-ray diffraction pattern of the aged sample  $\text{La}_{0.80}\text{Ba}_{0.20}\text{CoO}_3$  that gives the  $\rho$  versus  $T$  D curve shown in Fig. 2. From the crystallographic point of view the material has not deteriorated.

The materials that show the I-M-I sequence (samples A, B, and C) also display other interesting properties. If we measure their resistance at room temperature as a function of time using a constant current  $I^+$  in one

direction, initially we obtain a constant value of  $\rho_0^+$  during a  $t_1$ . A change in the direction of the current, now  $I^-$ , produces a change in the polarity of the electrodes and gives rise to a jump from  $\rho^+$  to other  $\rho^-$ . This behavior is expected in any resistance measured by this method. It is due to the presence of thermal EMFs effects in the welds because dissimilar materials are joined together. But while in other metallic and low-resistivity ( $\text{m}\Omega \text{ cm}$ ) semiconducting samples we observe a practically instantaneous change in the polarity, in the  $\text{La}_{0.80}\text{Ba}_{0.20}\text{CoO}_3$  sample when the initial polarity,  $I^+$ , is restored after  $t_2$ , an unexpected time dependent resistivity,  $\rho_t^+$ , different from  $\rho_0^+$ , is measured. After approximately 600 s  $\rho_0^+$  is recovered, as represented in Fig. 4. This effect is not present in samples without RSB.

To get a deeper insight into this peculiar behavior we also studied this phenomenon as a function of temperature. We took a sample showing the  $M-I$  transition (sample C in Fig. 2) and measured  $\rho^+(T)$  on cooling down. Apparently, the sample has a semiconductor behavior with two jumps at 175 K and 115 K, respectively (Fig. 5). Then, at 77 K, we changed the polarity of the current and  $\rho(T)$  was measured warming up. In this case the sample shows a semiconducting behavior from 77 to 115 K and metallic for  $T \text{ (K)} > 115$ , the positive slope of  $\rho(T)$  again changing at  $T_C = 175 \text{ K}$  (Fig. 5).

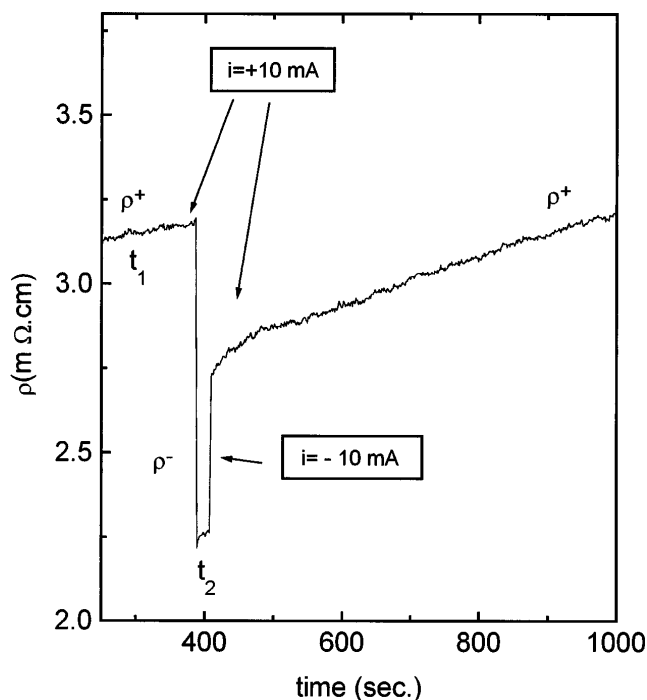


FIG. 4. Room temperature  $\rho$  versus time data of  $\text{La}_{0.80}\text{Ba}_{0.20}\text{CoO}_3$ . The figure shows the relaxation of  $\rho^+$  after having applied a +10 mA intensity during  $t_1 = 400 \text{ s}$  followed by a change in the polarity of the current to -10 mA for  $t_2 = 40 \text{ s}$  and finally restoring the initial +10 mA.

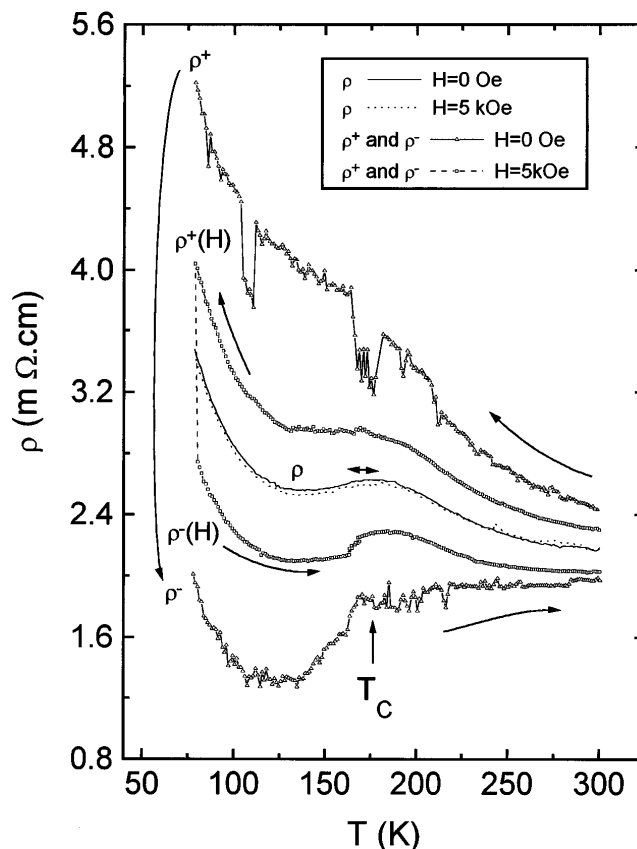


FIG. 5.  $\rho^+(H)$  versus  $T$ ,  $\rho^-(H)$  versus  $T$  and the average  $\rho(H)$  versus  $T$  curves corresponding to a sample of  $\text{La}_{0.80}\text{Ba}_{0.20}\text{CoO}_3$  with RSB (sample C in Fig. 2). The results of warming up applying  $-i$  ( $\rho^-$ ) and cooling down applying  $+i$  ( $\rho^+$ ) are represented by  $-\rho-$  when  $H = 0$  and by  $----$  when  $H = 5 \text{ kOe}$ .  $\rho(0)$  and  $\rho(5 \text{ kOe})$  are shown as a solid line and as dots, respectively.

When we measured  $\rho$  inverting the direction of the current at every temperature, as explained in the experimental section, we obtained the average  $\rho$  also represented in Fig. 5. A small thermal hysteresis was observed between the cooling down and warming up curves. In this case, we can observe that  $\rho$  lies approximately at the geometric average of  $\rho^+$  cooling down curve and  $\rho^-$  warming up curve.

To study the influence of  $H$  in these  $\rho(T)$  curves we measured  $\rho^+(T)$ ,  $\rho^-(T)$ , and  $\rho(T)$  under a field of  $H = 5 \text{ kOe}$ . The results are also plotted in Fig. 5.

An enlarged view of the effect of an  $H$  of 5 kOe on the  $\rho(T)$  curve can be seen in Fig. 6(a). At the temperature where separation between the  $\rho(5 \text{ kOe})$  and  $\rho(0)$  curves goes through a maximum,  $T = 135 \text{ K}$ , we measured the magnetoresistance of the sample: 2–3% [Fig. 6(b)]. A strong noise is noticeably observed in these measurements.

We also measured the effect of the field on the  $\rho(T)$  curve of the sample that does not show any more RSB (sample D in Fig. 2) and its magnetoresistance at 160 K [Figs. 7(a) and 7(b)]. In this case it is worth

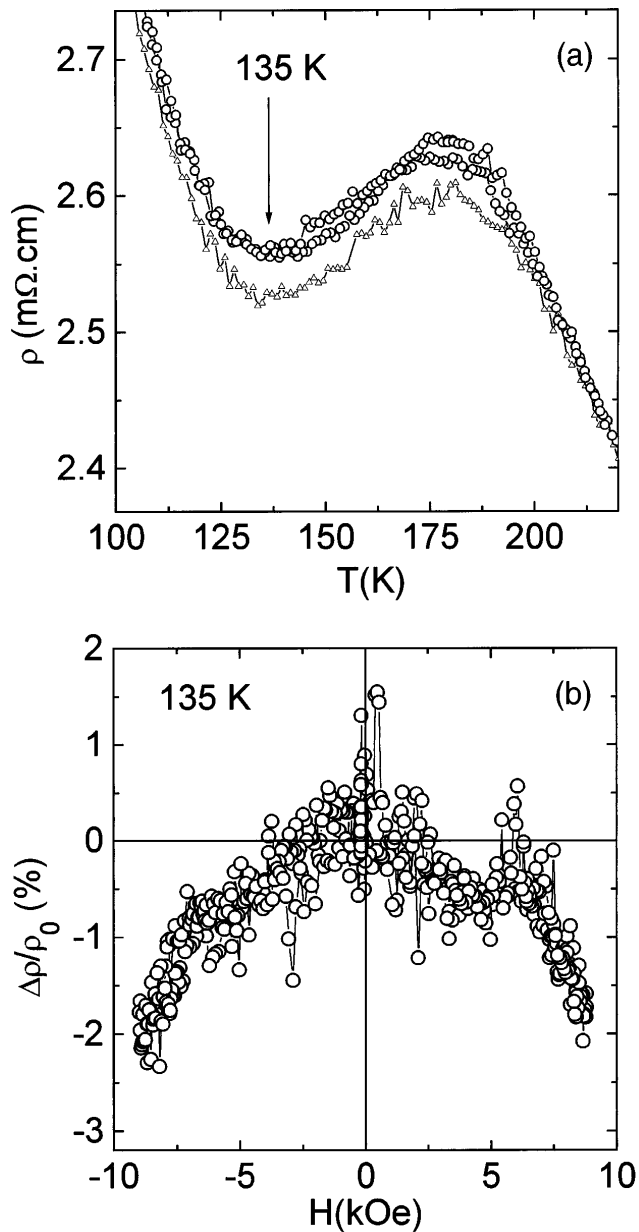


FIG. 6. (a) Enlarged view of the  $\rho(H)$  versus  $T$  data of sample C with RSB. Data corresponding to  $H = 0$  are represented by circles and those corresponding to  $H = 5$  kOe by triangles. The arrow shows the temperature at which the magnetoresistance was measured. It is plotted in part (b) of the figure.

noting that the noise is much lower than in the previous measurements and the differences between the warming up and cooling down curves (thermal hysteresis) are more clearly seen.

#### IV. DISCUSSION

We can summarize the phenomena reported by us in  $\text{La}_{0.80}\text{Ba}_{0.20}\text{CoO}_3$  in the semiconducting re-entrant region as (i) temporal evolution of  $\rho$  versus  $T$  curves, (ii) relaxation effects in its electrical resistivity and

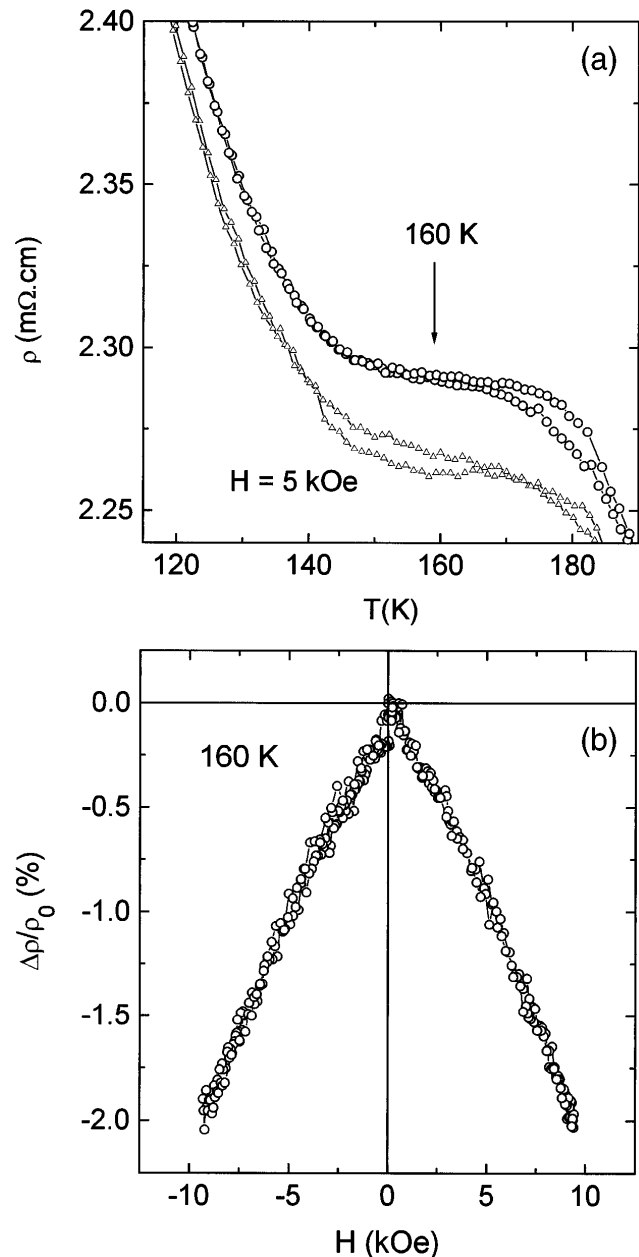


FIG. 7. (a)  $\rho(H)$  versus  $T$  data of sample D that has lost the RSB. Data corresponding to  $H = 0$  are indicated by circles and those corresponding to  $H = 5$  kOe are indicated by triangles. The temperature at which the magnetoresistance was measured is marked with an arrow. (b)  $\rho(H)$  of this sample at 160 K.

“diodic” behavior, (iii) resistivity fluctuations near the  $M - I$  transition, and (iv)  $\sim 2\text{--}3\%$  magnetoresistance for a field of 9 kOe, especially near  $T_{M1}$ .

In general, the behavior observed in these experiments can be understood as a result of segregation of two phases.<sup>1</sup> It has recently been proposed that in these cobalt perovskites there are two distinguishable electronic phases that coexist in the same crystallographic phase.<sup>12</sup> One would be hole-rich, metallic, and ferro-



magnetic, where the Co ions are in an intermediate spin configuration. The other would be hole-poor, semiconducting, and with antiferromagnetic exchange interactions, in which the Co ions are in a spin state that changes with temperature.<sup>12</sup>

In this  $\text{La}_{0.80}\text{Ba}_{0.20}\text{CoO}_3$  material the ferromagnetic phase has already reached the percolation threshold, so that bulk ferromagnetism is observed below  $T_C = 175$  K. Nevertheless, positive deviation from the Curie–Weiss law in the paramagnetic region is observed below 250 K. This deviation can be originated by the presence of magnetic short range order in small clusters above  $T_C$ .<sup>3</sup> The persistence of some of these superparamagnetic clusters above 250 K could be contributing to the enhanced effective magnetic moment ( $\mu_{\text{eff}} = 4.6 \mu_B$ ) observed with respect to the value ( $\mu_{\text{eff}} = 3.5 \mu_B$ ) found in equivalent cobalt systems.<sup>12</sup>

Alternating electrical conduction behaviors, I–M–I, that predominate in different temperature ranges reveals the presence of those two phases.

The predominant phase controls the electrical behavior defining the region with RSB. At low temperatures the metallic regions, which have not percolated yet, are disconnected so that the semiconducting behavior of the other phase is observed. Between  $T_{M11}$  and  $T_{M12}$  spin-state changes in that semiconducting phase allow the metallic, ferromagnetic clusters to percolate, and the spin-disorder scattering is the dominant mechanism. The temperature coefficient  $\partial\rho/\partial T$  changes its sign at the Curie point, thus indicating that the band structure is affected by the magnetic ordering. Above  $T_{M12}$  or  $T_C$ , the bulk system is paramagnetic, although small ferromagnetic clusters could be present with a very small conductivity, and the hole-poor phase dominates the electrical conduction that takes place by the movement of charge carriers through the semiconducting phase with an activated mobility.

Other support for the model of two electrically different phases coexisting in the system comes from the relaxation effects observed when the polarity of the current is changed and from its “dioidic” behavior. In this context, a ferroelectric field effect in epitaxial heterostructures of  $\text{Pb}(\text{Zr}_{0.52}\text{Ti}_{0.48})\text{O}_3$  (PZT)/ $\text{SrRuO}_3$  has recently been reported.<sup>13</sup> In these heterostructures, the ferroelectric polarization of PZT induces a nonvolatile change in the carrier density of the adjacent metallic ferromagnetic  $\text{SrRuO}_3$  perovskite layer, giving rise to a change in its resistivity. This change of  $\rho$  was nonvolatile for a period of several days.

A similar phenomenon can be occurring in these RSB samples. If these materials are thought of as an electrical inhomogeneous medium, where some metallic clusters are covered with a semiconducting and dielectric material, the change in the polarity of electrodes will affect the charge distribution in the dielectric medium.

This, in turn, will change the density of charge carriers and therefore  $\rho$ . With time, as the charge distribution in the semiconducting media evolves toward the original configuration, the resistivity tends to its initial  $\rho_0$  value.

Within this model of two distinguishable electronic phases coexisting within the same crystallographic phase, the resistivity fluctuations observed in our measurements near the  $M - I$  transition (which are much larger than those found in related systems such as CMR  $\text{La}_{2/3}\text{Ca}_{1/3}\text{MnO}_3$ <sup>14</sup>) could originate in fluctuations of the magnetization in the ferromagnetic clusters. Nevertheless, we can not discard the fact that grain boundaries can also be playing an important role in such behavior. In this context, it is well known that typical grain boundary phenomena such as segregation, oxygen nonstoichiometry, other complex defects, etc.,<sup>15</sup> can greatly affect the sample resistivity.<sup>16</sup> In this case, defect motion at the grain boundaries would produce microscopic inhomogeneities in the material that could give rise to inhomogeneities in its electrical transport, this contributing to the observed noise enhancement near the  $M - I$  transition.

As for magnetoresistance in cobalt perovskites, several authors have recently reported magnetoresistance in La–Sr–Co–O perovskites<sup>17,18</sup> and have proposed their application as a magnetic field sensor.<sup>19</sup>

The 2–3% magnetoresistance shown by these  $\text{La}_{0.80}\text{Ba}_{0.20}\text{CoO}_3$  samples at temperatures near  $T_{M11}$  and  $T_{M12}$  for a field as low as 9 kOe could be interpreted as the result of growth of the hole-rich ferromagnetic regions under the application of the field at the expense of the poor-conducting matrix, through changes in its Co-spin state. These values of magnetoresistance would be a promising result if the noise did not affect the measurements so much. This can be a serious drawback for the possible use of these materials as magnetic sensors.

As for the observed electrical “aging” and evolution with time, it could be related to small changes in the oxygen stoichiometric of the sample. This assumption is supported by preliminary oxygen analyses,<sup>20</sup> by the fact that appropriate thermal treatments that allow the sample to recover its oxygen content<sup>20</sup> can restore the initial  $\rho$  versus  $T$  curve, and by results reported by other authors on the evolution from metallic to semiconducting behavior of  $\text{La}_{1-x}\text{Sr}_x\text{CoO}_3$  thin films.<sup>21</sup>

Finally, it is worth mentioning that the reported effects of temporal evolution, relaxation effects, and fluctuation in its electrical resistivity, as well as its “dioidic” behavior are not restricted to this barium-doped material. We have also observed it in other polycrystalline cobalt perovskites that we have prepared by different routes and with different particle size,<sup>22</sup> and that also show RSB behavior:  $\text{La}_{1-x}\text{Sr}_x\text{CoO}_3$  ( $x = 0.20, 0.25$ ) and  $\text{La}_{0.70}\text{Ca}_{0.30}\text{CoO}_3$ .<sup>20</sup>

More work is in progress to try to completely clarify these surprising and interesting effects and to fully separate the intragranular and intergranular contributions to the observed electrical properties.

## ACKNOWLEDGMENT

The authors are grateful for the financial support from DGICYT, Ministerio de Educación y Ciencia, Spain, under Project MAT98-0416-C03-02.

## REFERENCES

1. E. L. Nagaev, Phys. Status Solidi (B) **186**, 9 (1994) and references therein.
2. J. B. Goodenough J-S. Zhou, and K. Allan, J. Mater. Chem. **1**, 715 (1991).
3. J. M. de Teresa, M. R. Ibarra, P. A. Algarabel, C. Ritter, C. Marquina, J. Blasco, J. García, A. del Moral, and Z. Arnold, Nature **386**, 256 (1997).
4. L. I. Koroleva, R. V. Demin, and A. M. Balbashov, JETP Lett. **65**, 474 (1997).
5. H. L. Ju and Hyunchul Sohn, J. Mag. Mater. **167**, 200 (1997).
6. W. C. Koehler and E. O. Wollan, J. Phys. Chem. Solids **2**, 100 (1957).
7. P. M. Raccach and J. B. Goodenough, Phys. Rev. **155**, 932 (1967).
8. J. B. Goodenough, J. Phys. Chem. Solids **6**, 287 (1958).
9. M. A. Señas-Rodríguez and J. B. Goodenough, J. Solid State Chem. **116**, 224 (1995).
10. G. H. Jonker and J. H. van Santen, Physica **19**, 120 (1953).
11. J. B. Goodenough, Mater. Res. Bull. **6**, 967 (1971).
12. M. A. Señas-Rodríguez and J. B. Goodenough, J. Solid State Chem. **118**, 323 (1995).
13. C. H. Ahn, R. H. Hammond, T. H. Geballe, M. R. Beasley, J. M. Triscone, M. Decroux, O. Fisher, L. Antognazza, and K. Char, Appl. Phys. Lett. **70**, 206 (1997).
14. H. T. Hardner, M. B. Weissman, M. Jaime, R. E. Treece, P. C. Dorsey, J. S. Horwitz, and D. B. Chrisey, J. Appl. Phys. **81**, 272 (1997).
15. *Ceramic Materials for Electronics, Processing, Properties and Applications*, 2nd ed., edited by Relva C. Buchanan (Marcel Dekker, New York, 1991).
16. J. Nowotny and M. Rekas, Ceram. Int. **17**, 227 (1991).
17. V. Golovanov, L. Mihaly, and A. R. Moodenbaugh, Phys. Rev. B **53**, 8207 (1996).
18. R. Mahendiran and K. Raychaudhuri, Phys. Rev. B **54**, 16044 (1996).
19. R. Mahendiran, K. Raychaudhuri, A. Chainani, and D. D. Sarma, Rev. Sci. Instrum. **66**, 3071 (1995).
20. M. Sánchez, C. Rey, M. P. Breijo, M. A. Señas-Rodríguez, S. Castro, J. Mira, R. D. Sánchez, and J. Rivas, unpublished results.
21. R. Ramesh, A. Krishnan, D. Keeble, and E. Poindexter, J. Appl. Phys. **81**, 3543 (1997).
22. M. A. Señas-Rodríguez, M. P. Breijo, S. Castro, J. Mira, R. D. Sánchez, and J. Rivas, Bol. Soc. Esp. Cerám. Vidrio **37**, 25 (1998).